Paper ID: AM-13

Improvement of Vibration Isolation Characteristics using Acceleration Feedback Based on Kalman Filter Estimation

M. M. Zaglul Shahadat[1], T. Mizuno[2], Y. Ishino[2], and M. Takasaki[2]
[1] Graduate School of Science & Engineering, Saitama University
[2] Department of Mechanical Engineering, Saitama University
E-mail: shahadat230@yahoo.com

Abstract

A horizontal vibration isolation system utilizing displacement cancellation technique is studied both analytically and experimentally. The isolation and middle tables of the investigated vibration isolation system, involving displacement cancellation technique, are controlled by an infinite stiffness control and positive stiffness control, respectively. In this study, the dynamic characteristics of the vibration isolation system are improved by adding acceleration feedback to the original controllers. MEMS (Micro Electrical Mechanical System) accelerometers are used to measure acceleration for the feedback. Since the acceleration measured by a MEMS accelerometer usually contains undesired noise, the estimated acceleration by Kalman Filter (KF) is used instead of the measured value in the acceleration feedback. The dynamic responses of the system are investigated with the acceleration feedback based on the KF estimation and the measured signal individually. The experimental results show that the KF-estimated acceleration feedback improves the vibration isolation characteristics significantly.

Keywords: *Active control, Vibration isolation, Infinite stiffness, Zero compliance, Acceleration feedback.*

1. Introduction

Nowadays, the position accuracy in Hi-tech manufacturing process has progressed to nanometer range. A small scale disturbance in high precision production site may hamper the system to acquire the desired accuracy. In most silicon wafer and semiconductor industries, the accuracy is a key performance objective. Thus, the demand for high performance vibration isolation system is increasing recently in various industrial sectors such as semiconductor industries, silicon wafer industries and so on. There are two main sources of vibration: (1) vibration transmitted from ground (ground vibration) through suspension and (2) vibration caused by disturbances acting on vibration isolation table directly (direct disturbance). A vibration isolation system should be able to suppress simultaneously both disturbances.

Low-stiffness systems are better for attenuating ground vibration, whereas high-stiffness systems are suitable for direct disturbance [1]. In addition, a trade-off regarding high stiffness and low stiffness is inevitable in conventional passive type vibration isolation systems. In contrast, active vibration isolation systems, in principle, are not vulnerable with respect to this difficulty [2]. Consequently, the active micro-vibration isolation technology has recently received satisfactory emphasis in the Hi-tech industries [2-4].

To acquire high stiffness and low stiffness simultaneously by a single active vibration isolation unit, the mechanism, involving two series connected isolators, was proposed [5-6]. Mizuno *et al*. have applied negative stiffness technique to isolate vibration using two isolators connected in series [5-6], where one isolator is controlled to have negative stiffness and the other has positive stiffness of same amplitude. First, a zero-power control magnetic suspension system was connected with a normal spring in series [5]. Zero-power control magnetic suspension systems have itself unique characteristic that they behave as if they have negative stiffness. Mizuno *et al*. acquired a vertical vibration isolation system by a linear actuator connected with a normal spring in series, where the linear actuator was controlled with proper negative stiffness controller [6], and the characteristics of this system was further improved by using positive stiffness actuator instead of the normal spring [7]. However, in practice, it is often difficult to maintain equal absolute stiffness of both isolators, and unequal stiffness of the isolators in negative stiffness technique hampers the vibration isolation system to obtain zero compliance. The vibration isolation system using a displacement cancellation technique can overcome this problem [8] because the displacement cancellation control focuses on the displacement rather than the stiffness of the isolator.

Mizuno *et al*. developed a horizontal vibration isolation system using displacement cancellation control [8], where an integral-controlled linear actuator is connected with a normal spring in series. The authors have developed a three-axis horizontal vibration isolation system using this technique, where voice coil motors (VCMs) are used as actuators. Nevertheless, the transient response is still a problem of the aforementioned system and should to be improved. A feedforward control can reduce the transient displacement. To realize a feedforward control, however, the prediction of the disturbances is necessary although in most cases the disturbances are unpredicted.

In this paper, an acceleration feedback is added to the controllers to improve such vibration isolation characteristics for unknown disturbances. In the experiment, MEMS accelerometers are used instead of servo-accelerometer to measure acceleration. An advantage of MEMS is low in cost. However, the output signal of MEMS accelerometers includes undesirable noise. To reduce such noise from the measured signal, various filter techniques are available, and one of them is Kalman Filter (KF). The KF performs suitably to improve the accuracy of the rotor position in active magnetic bearings [9]. In this study, the acceleration feedback based on KF-estimation instead of direct measured acceleration is used to avoid the noise in the measured acceleration.

2. Displacement cancellation technique to isolate vibration and developed system

The zero-compliance against direct disturbance and the soft suspension against ground vibration are two required criteria for a vibration isolation system. In this study, a displacement cancellation technique is applied to realize these two criteria simultaneously in a horizontal vibration isolation system. In the following, the concept of the displacement cancellation technique is presented.

The displacement cancellation technique comprises from two series connected isolators, one of which is a soft spring and the other is controlled to cancel displacement of the spring as shown in Fig. 1. Because stiffness k_1 is positive, the displacement of the isolation table $\bar{y}$ against a direct disturbance is cancelled by the upper isolator (Fig. 1) with the I-PD (integral-proportional derivative) control; the upper portion behaves as itself has negative stiffness. The displacement $\bar{y}$ can be expressed as

$$\bar{y} = (y_1 + y_2) - (y_1 - \Delta y_1 + y_2 - \Delta y_2)\,, \tag{1}$$

where Δy_1 and Δy_2 respectively indicate the displacements of the lower and upper portions, respectively. The resultant displacement of the upper mass would be zero when following condition is satisfied:

$$0 = (y_1 + y_2) - (y_1 - \Delta y_1 + y_2 - \Delta y_2), \Rightarrow \Delta y_1 = -\Delta y_2 = \Delta y\,. \tag{2}$$

Equation (2) indicates that zero-compliance against direct disturbance takes place in the series combination of two isolators (Fig. 1) when contraction in one isolator is absolutely equal to the extraction in the other isolator.

For ground vibration, meanwhile, the combination of the middle mass and spring works as a mechanical filter that attenuates the transmission of vibration to the isolation table. In addition, an electric filter should be inserted into the feedback loop from the displacement of the middle mass to the actuator for improving the vibration isolation performance. A simple structural diagram of a horizontal vibration isolation system using this concept is shown in Fig. 2. For the developed system, the middle mass is suspended from the base through actuators (VCM) with PD (proportional derivative) control and the isolation table is mounted on the middle table through actuators (VCM) with I-PD control. A photograph of the developed horizontal vibration isolation system is shown in Fig. 3.

Moreover, to improve the dynamic responses of the system against unpredicted disturbances, two MEMS accelerometers are individually attached with two moving table of the developed system. MEMS accelerometers which are usually small in size can be placed in any part of the system. In addition, the acceleration signals measured by MEMS are estimated by the Kalman filter (KF) for improving the signal quality before being used in the acceleration feedback.

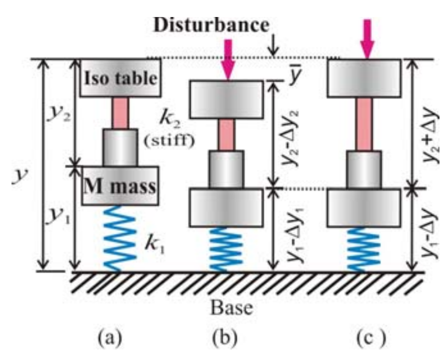

Fig. 1 Concept of displacement cancellation technique

3. Control system design

Basic equation

A basic model of a single-degree-of-freedom horizontal vibration isolation system is shown in Fig. 4, and the controllers will be designed based on this model. The basic motion equation of the table can be written as follows:

$$m\ddot{x} = f_a \,, \tag{3}$$

where

m: mass of the table,

x: displacement of the table along x-axis,

f_a: actuator's thrust force.

The thrust force f_a is proportional to coil current i as expressed by

$$f_a = k_i i \,, \tag{4}$$

where k_i is the thrust force coefficient of the actuator. The Laplace transforms of Eqs. (3) and (4) yield the transfer function representation written as

$$X(s) = \frac{k_i}{ms^2} I(s) \,, \tag{5}$$

where each Laplace-transform variable is denoted by its capital.

Design of infinite stiffness controller including acceleration feedback

The isolation table is guided with I-PD control and is presented by block diagram shown in Fig. 5. The I-PD control operates to cancel the relative displacement of the table using a command signal r; hence, the control current for the I-PD control can be expressed as follows:

$$i = -P_z \int (x - r)dt - P_d x - P_v \dot{x} - P_a \ddot{x} \,, \tag{6}$$

where P_d, P_v, P_z and P_a denote proportional, derivative, integral and acceleration feedback gains of the controller, respectively. The Laplace-transform of Eq. (6) becomes

$$I(s) = \frac{P_z}{s} r(s) - \frac{P_z}{s} X(s) - P_d X(s) - P_v sX(s) - P_a s^2 X(s) \,. \tag{7}$$

Substituting of Eq. (7) into Eq. (5) leads to the transfer function representation of the I-PD controlled system represented as

$$\frac{X(s)}{R(s)} = \frac{\hat{t}_n(s)}{\hat{t}_c(s)} \,, \tag{8}$$

where the numerator part is given by $\hat{t}_n(s) = \dfrac{k_i P_z}{(m + k_i P_a)}$. In Eq. (8), $\hat{t}_c(s)$ indicates the characteristic equation of the system (Fig. 4) with an acceleration feedback, which is given by

$$t_c(s) = s^3 + \frac{k_i P_v}{m + k_i P_a} s^2 + \frac{k_i P_d}{m + k_i P_a} s + \frac{k_i P_z}{m + k_i P_a} \,. \tag{9}$$

Equation (9) indicates that this system is a 3rd-order system. The characteristic equation of a 3rd-order ideal system is supposed to be represented as

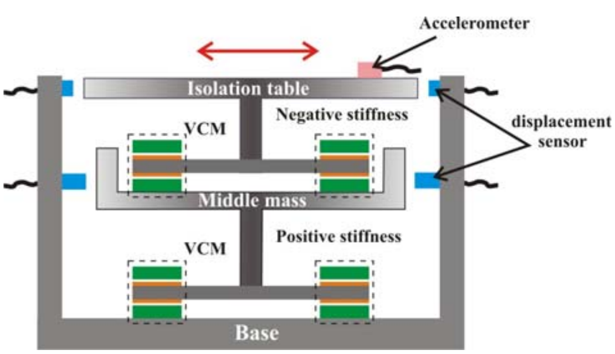

Fig. 2 Structure of horizontal vibration isolation system

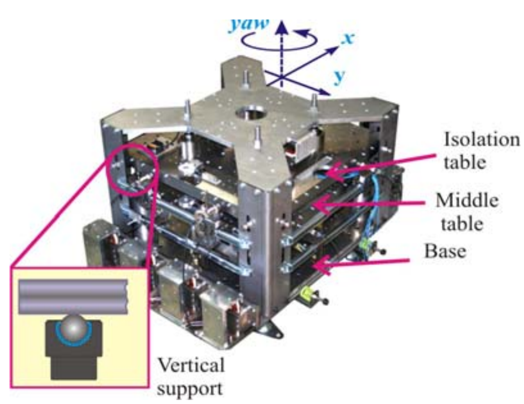

Fig. 3 Photograph of the developed system

$$t_d(s) = (s^2 + 2\zeta_1\omega_1 s + \omega_1{}^2)(s + \omega_2) = s^3 + \alpha_2 s^2 + \alpha_1 s + \alpha_0 . \quad (10)$$

According to the pole assignment method, the controller gains (P_d, P_v, P_z) are determined uniquely by matching of the coefficients of Eqs. (9) and (10) as

$$P_z = \frac{\alpha_0}{k_i}(m + k_i P_a), \quad P_d = \frac{\alpha_1}{k_i}(m + k_i P_a), \quad P_v = \frac{\alpha_2}{k_i}(m + k_i P_a) ,$$

where $\alpha_2 = 2\zeta_1\omega_1 + \omega_2$, $\alpha_1 = 2\zeta_1\omega_1\omega_2 + \omega_1{}^2$, $\alpha_0 = \omega_1{}^2\omega_2$. The theoretical analysis outlined above shows that the addition of an acceleration feedback increases the mass of the system virtually, and a heavy system has smaller displacement than to a light system for the same disturbance. Hence, the acceleration feedback can improve the dynamic responses of a vibration isolation system. However, in practice, the system would be unstable if the value of P_a is too large beyond a certain range. In experiment, the value of P_a is selected so that the system maintains stability.

4. Optimum acceleration estimation using Kalman filter

The acceleration signal measured by a MEMS accelerometer usually contains undesirable high frequency noise. There are several methods to reduce the noise level from a signal. In this study, the KF is used to deduct noise from the measured acceleration signal and this KF-estimated acceleration is for utilized realizing the acceleration feedback in the controlled system. The KF used in this study is an observer based filter, which estimates the signals by minimizing mean-square estimation errors and shown in Fig. 6. The KF algorithm comprises two steps; (i) prediction of states, and (ii) updating of the predicted states.

The state space theoretical model of the system (Fig. 4) including process noise (w) and measurement error (v) can be represented as follows:

$$\dot{\boldsymbol{X}} = \boldsymbol{A}\boldsymbol{X} + \boldsymbol{B}F_d + \boldsymbol{w} , \quad (11)$$

$$\boldsymbol{y} = \boldsymbol{C}\boldsymbol{X} + \boldsymbol{v} , \quad (12)$$

The discrete formats of Eqs. (11) and (12) are given in below which are used in the KF algorithm with sampling time Δt.

$$\overline{\boldsymbol{X}}_T = \boldsymbol{\varphi}\hat{\boldsymbol{X}}_{T-1} + \boldsymbol{B}.\Delta t F_d + \Delta t.\boldsymbol{w} , \quad (13)$$

$$\boldsymbol{y} = \boldsymbol{C}\overline{\boldsymbol{X}}_T + \boldsymbol{v} , \quad (14)$$

where $\boldsymbol{\varphi} = \boldsymbol{A}.\Delta t + .\boldsymbol{I}$, $\overline{X}$ and $\hat{X}$ define predicted and estimated value of X, respectively. The subscript T denotes the time step. The discrete KF algorithm is given as follows:

Predicted step

$$\overline{\boldsymbol{X}}_{T-1} = \varphi\hat{\boldsymbol{X}}_{T-1} + \boldsymbol{B}u , \quad (15)$$

$$\overline{\boldsymbol{P}}_{T-1} = \varphi\hat{\boldsymbol{P}}_{T-1}\varphi' + \boldsymbol{Q} . \quad (16)$$

Updated state

$$\hat{\boldsymbol{X}}_T = \overline{\boldsymbol{X}}_{T-1} + \boldsymbol{K}_T(y_T - \boldsymbol{C}\overline{\boldsymbol{X}}_{T-1}) , \quad (17)$$

$$\boldsymbol{K}_T = \left(\overline{\boldsymbol{P}}_{T-1}\boldsymbol{C}'\right) / \left(\boldsymbol{C}\overline{\boldsymbol{P}}_{T-1}\boldsymbol{C}' + \boldsymbol{R}\right), \quad (18)$$

$$\hat{\boldsymbol{P}}_T = (\boldsymbol{I} - \boldsymbol{K}_T\boldsymbol{C})\hat{\boldsymbol{P}}_{T-1} . \quad (19)$$

where $\boldsymbol{A}$: state transition matrix, $\boldsymbol{B}$: control input matrix, $\boldsymbol{C}$: measurement matrix, $\boldsymbol{Q}$: process noise covariance

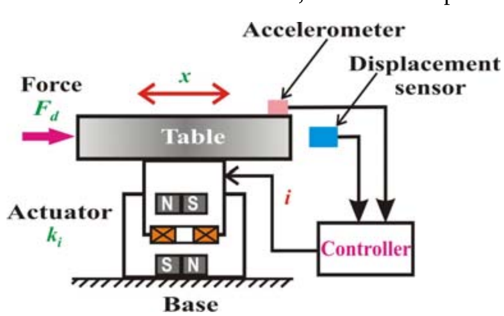

Fig. 4 Basic model of single axis control system

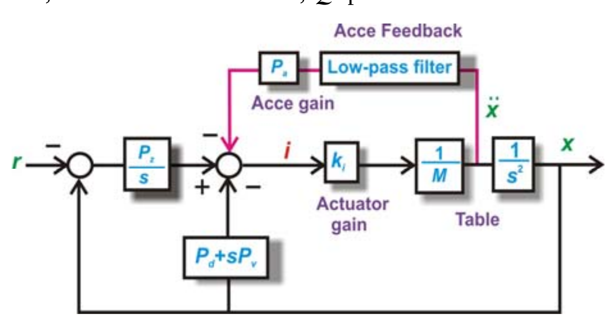

Fig. 5 I-PD controller with acceleration feedback

matrix, ***R***: measurement covariance matrix, ***K***: Kalman gain matrix, ***X***: states matrix, ***P*** : covariance matrix of error in estimation. The influences of the KF on the control system are studied by numerical simulations. It is assumed that the control system is subject to a white Gaussian noise. Figure 7 shows the simulation results. The simulations are conducted for (i) control based on the KF estimation and (ii) control based on direct measured signal. It is observed that the KF can appropriately estimate the measured signal with low levels of noise as shown in the upper chart. Moreover, the control based on the measured displacement signal makes the object being deviated highly. On the other hand, the control based on KF-estimated displacement signal decreases the control deviation significantly.

5. Experimental results and discussions

In the experiments, the frequency responses to direct disturbance of the developed system are measured. To generate direct disturbances on the isolation table, two VCMs are mounted on the isolation table and fixed respect to the base. Moreover, to compare the dynamic responses, the responses of the developed system with and without acceleration feedback are drawn in the same graph. At the same time, the effect of the KF-estimated acceleration feedback on the behaviors of the developed system is investigated.

The displacement gains and phase angles of the isolation table with respect to the frequency of applied direct disturbance are shown in Fig. 8. The responses are measured for both with and without the acceleration feedback to the controller. The individual and combined effects of the acceleration feedback of the isolation table and middle table on the behaviors of the developed system are investigated. It is found that the addition of acceleration feedback with the original controller improves the vibration isolation behaviors. The controller gains are kept constant through the experiments, where the value of P_a is chosen 0.2 (As^2/m) for both tables.

In theoretical analysis, it was observed that the larger acceleration feedback gain (P_a) causes the improvement of vibration isolation characteristics (Eq. (8)). This theoretical finding is confirmed by experimental results shown in Fig. 9. In Fig. 9, the frequency responses of the isolation table with varying P_a (0.2 to 0.4 As^2/m) are shown. Because the poles of the controlled system depend on the value of P_a, the gains of the controller are reselected to keep the same poles in these experiments.

The effect of acceleration feedback based on KF estimation on the frequency responses to direct disturbance of the isolation table is shown in Fig. 10. It is observed that the acceleration feedback based on the KF estimation can reduce the gain by 6% at a resonance frequency respect to no acceleration feedback. The KF algorithm produces an estimated output that depends on the average value of previous successive outputs. Therefore, it has less possibility to have two successive signals which are very different in magnitude in the KF-estimated signals. This may one of the reasons for improvement in vibration isolation characteristics using KF.

6. Conclusion

The horizontal vibration isolation system with displacement cancellation technique was studied. The acceleration feedback added to the original controllers improved the dynamic characteristics of the vibration isolation system. In this investigation, the MEMS accelerometers were used to measure acceleration. The KF was used to decrease the levels of noise in the acceleration signal measured by MEMS accelerometer. From the experimental results, it was observed that the acceleration feedback based on the KF estimation decreased the peak gain by 6% compared to that without acceleration feedback.

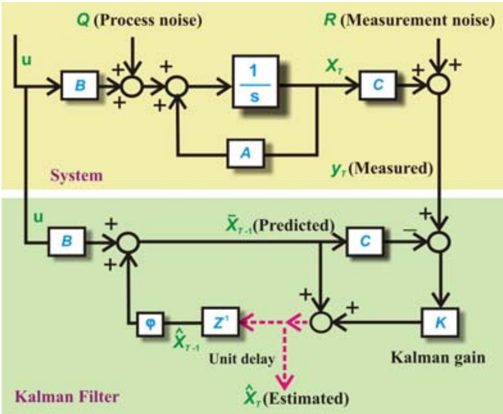

Fig. 6 KF algorithm by block diagram

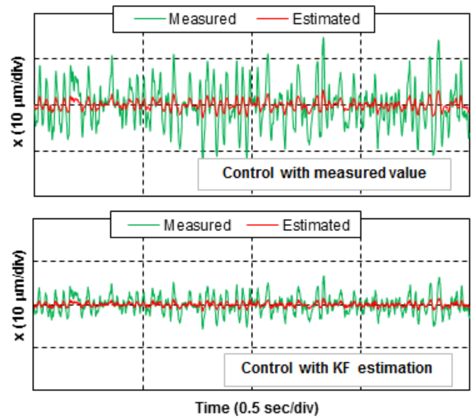

Fig. 7 Noise reduction and system behavior with KF (simulated)

6. References

[1] M. Yasuda, and M. Ikeda, "Double-Active Control of Micro vibration Isolation Systems to Improve Performances (Application of Two-Degree-of-Freedom Control)". *Transaction of Japan Society of Mechanical Engineers*, C, 59,562, pp.1694-1701, 1993.

[2] E. I. Rivin, "Vibration Isolation of Precision Equipment," *Precision Engineering*, vol. 17, pp. 41-56.

[3] C. R. Fuller, S. J. Elliott, and P. A. Nelson, "Active Control of Vibration", *Academic Press*, , 1996, pp. 213-220,1995.

[4] D. L. Trumper, and T. Sato, "A Vibration Isolation Platform," *Mechatronics*, vol. 12, pp. 281-294, 2002.

[5] T. Mizuno, M. Takasaki, D. Kishita, and K. Hirakawa, "Vibration Isolation System Combining Zero-Power Magnetic Suspension with Springs", *Control Engineering Practice*, Vol.15, No.2, pp 187-196, 2007.

[6] T. Mizuno, T. Toumiya, and M. Takasaki, "Vibration Isolation Using Negative Stiffness", *JSME International Journal*, Series C, vol. 46, (3), pp. 807-812, (2003).

[7] Md. E. Hoque, M. Takasaki, Y. Ishino, and T. Mizuno, "Development of a Three-Axis Active Vibration Isolator Using Zero-Power Control", IEEE/ASME Transactions on Mechatronics, vol. 11, no. 4, pp.462-470, 2006.

[8] T. Mizuno, T. Furushima, Y. Ishino, and M. Takasaki, "Realization of Zero-Compliance System by Using Displacement Cancellation Control", *Journal of Vibration and Control*, vol. 16(4), pp. 585-599, 2010.

[9] T. Schuhmann, W. Hofmann, and R. Werner, "Improving Operational Performance of Active Magnetic Bearing Using Kalman Filter and State Feedback Control", *IEEE Transactions on Industrial Electronic*, vol. 59, no. 2, pp. 821-829, 2012.

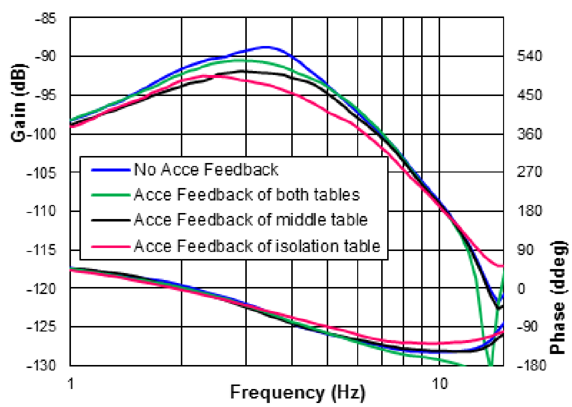

Fig. 8 Effect of Acceleration feedback on frequency response (isolation table) to direct disturbance

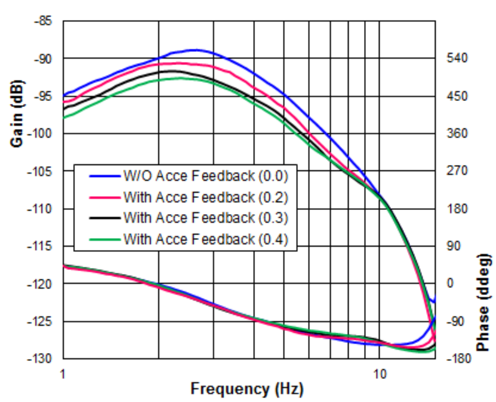

Fig. 9 Frequency responses for different acceleration feedback gain

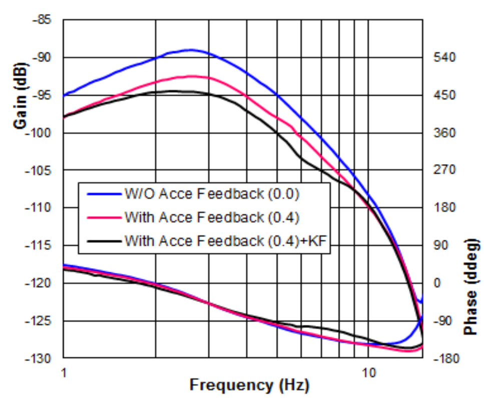

Fig. 10 Effect of KF estimated acceleration feedback